



Potential predictability of boreal winter precipitation over central-southwest Asia in the North American multi-model ensemble

Muhammad Azhar Ehsan^{1,2} · Fred Kucharski^{1,2} · Mansour Almazroui²

Received: 24 August 2018 / Accepted: 1 October 2019 / Published online: 8 October 2019
© Springer-Verlag GmbH Germany, part of Springer Nature 2019

Abstract

The potential predictability and skill of boreal winter (December to February: DJF) precipitation over central-southwest Asia (CSWA) is explored in six models of the North American Multimodel Ensemble project for the period 1983–2018. The seasonal prediction data for DJF precipitation initialized at Nov. (Lead-1) observed initial condition is utilized. The potential skill is estimated by perfect model correlation (PMC) method, while observed real skill is calculated by the temporal anomaly correlation coefficient (TCC). The main focus is over the Northern Pakistan (NP: 68°–78°E, 31°–37°N), which is a dominant winter precipitation sub-region in CSWA. All participating models generally capture the observed climatological pattern and variation in winter precipitation over the region. However, there are some systematic biases in the prediction of the climatological mean DJF precipitation, specifically an overestimation of precipitation over the foothills of the Himalayas in all models. The substantial internal atmospheric variability (noise) in the seasonal mean (signal) means that the regional winter precipitation is poorly predictable. The NCEP climate forecast system (CFSv2) and two Geophysical Fluid Dynamics Laboratory models (FLOR-A and FLOR-B) show the lowest potential and real skill. The COLA and NASA models show moderate but statistically significant PMC and TCC values. Each model captures the observed relationship between spatially averaged DJF precipitation over NP, with sea surface temperature (SST) and 200 hPa geopotential height (Z200), in varying details. The COLA and NASA models skillfully matched the observed teleconnection patterns, which could be a reason for their good performance as compared to other models. It also found that SSTs in the tropical oceans are relatively well predicted by NASA model when compared with other models. A critical outcome of the predictive analysis is that the multimodel ensemble (MME: A combination of six models and 79 members) does not show many advantages over the individual models in predicting boreal winter precipitation over the region of interest. Together, these results indicate that reliable prediction of the boreal winter precipitation over CSWA remains a big challenge in initialized models.

Keywords South Asia · Pakistan · HKH range · NMME · Predictability · Skill

1 Introduction

The agriculture production and many other economic activities of central-southwest Asia (CSWA) heavily depend on precipitation anomalies especially in Northern Pakistan (NP), the primary agriculture zone and food basket of

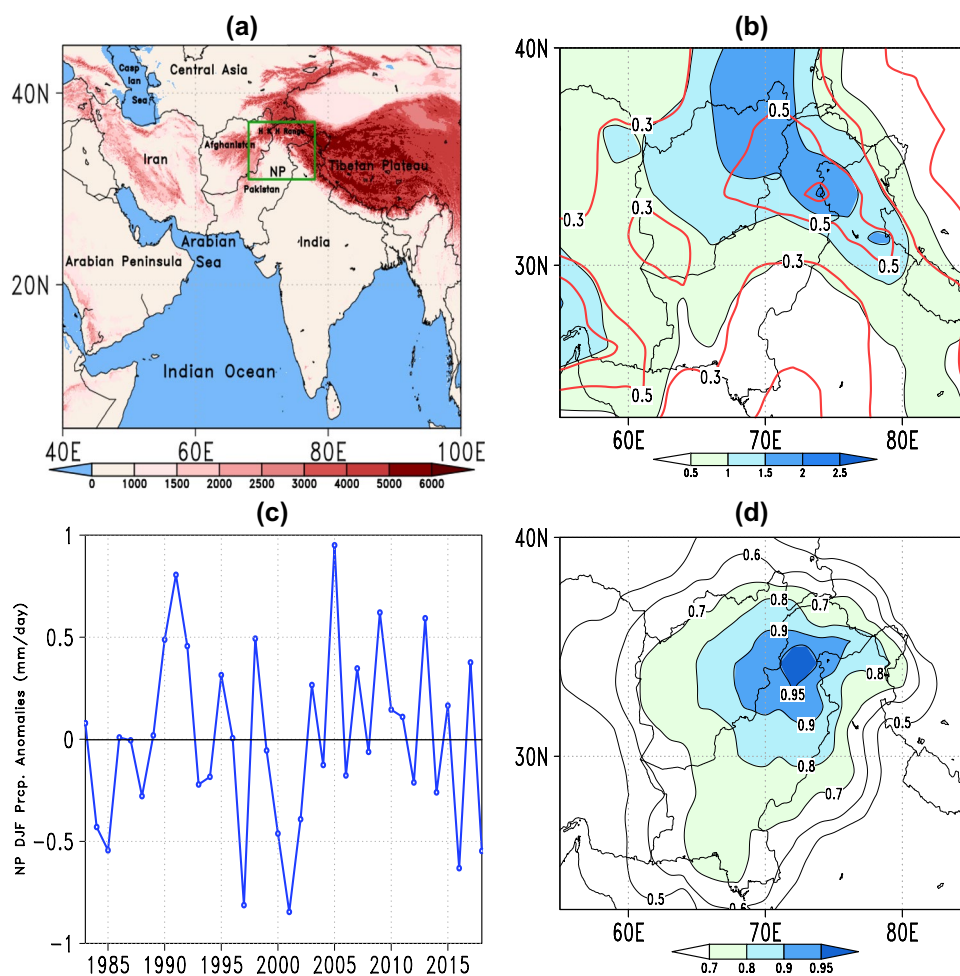
more than 200 million people (Rehman et al. 2016; Adnan et al. 2017). Northern Pakistan has very complex topography (Fig. 1a), and the mean boreal winter precipitation and its variability are strictly related to the orientation and elevation of the mountain ranges existing in the region: the Himalaya-Karakoram-Hindukush is collectively known as the HKH range (Palazzi et al. 2013). A substantial fraction of the boreal winter precipitation falls along the slopes of the HKH in the form of snow (Immerzeel et al. 2015). The subsequent melting of this winter snow during next summer is the most significant source of water (Lutz et al. 2014) for “Kharif” crops like rice that need ample water for its cultivation. The region’s lower latitudes also receive a good amount of winter rainfall (Sarfaraz and Khan 2015), which

✉ Muhammad Azhar Ehsan
mehsan@ictp.it; azhar.ehsan82@gmail.com

¹ Earth System Physics Section, The Abdus Salam International Centre for Theoretical Physics (ICTP), Trieste, Italy

² Center of Excellence for Climate Change Research (CECCR), King Abdulaziz University, Jeddah, Saudi Arabia

Fig. 1 **a** Core region (NP: 68°–78°E, 31°–37°N) of winter (DJF: Dec–Jan–Feb) precipitation and its neighborhoods. Topography of the region is indicated by the colors, with high elevation in red and lower elevations in beige. **b** Spatial DJF mean precipitation climatology (shaded) and standard deviation (contour). **c** The spatially averaged DJF precipitation time series over NP for 36-years (1983–2018). **d** The correlation of the NP precipitation time series to the precipitation anomalies during DJF. In **d** a correlation coefficient higher than 0.32 is statistically significant at 5% confidence level, using a *t* test. Unit of precipitation and elevation are mm day⁻¹ and meter respectively



is critical for “Rabi” crops like wheat that are sown during October through December and are harvested during March and April.

The influence of El Niño Southern Oscillation (ENSO) is one of the most critical factors that modulate the CSWA precipitation anomalies during boreal winter (Barlow et al. 2002; Hoell et al. 2014, 2015a; Cannon et al. 2016). For regional climate predictions, understanding of the ENSO connection to a regional climate is essential, as most of the climate prediction signal in current operational prediction systems arise from ENSO (Palmer et al. 2004; Wang et al. 2009; Kirtman et al. 2014; Hoell et al. 2017a, 2018a). Severe persistent drought is a prominent feature of the CSWA hydro-climatology (Barlow et al. 2002, 2016; Hoell et al. 2013b, 2017a), therefore accuracy in prediction of the boreal winter precipitation has great value, which can inform the concerned government agencies and stakeholders to cope with the adverse consequences of precipitation variability, particularly during drought condition.

Coupled global climate models (CGCMs) have become useful tools to make forecasts at multiple timescales (Dunstone et al. 2016) ranging from sub-seasonal to seasonal

(S2S) and seasonal to decadal (S2D) for climate-sensitive sectors (Schepen et al. 2016) such as water resources management (Viel et al. 2016; Arnal et al. 2017), agriculture (Ogutu et al. 2018) and energy production (Clark et al. 2017). While the CGCMs have demonstrated advanced configurations and more realistic representation of the earth system, the skill of a seasonal forecast system strongly depends on the model parameterizations (Ehsan et al. 2017b) and its initialization strategy (Xue et al. 2011; Barnston and Tippet 2013), and also varies according to variable, region, season, and lead-time (Saha et al. 2016; Almazroui et al. 2017; Ehsan et al. 2017a, 2019).

One fundamental question in seasonal climate forecasting is whether one prediction system is more skillful than another. A wide range of seasonal climate predictability studies has been conducted previously by using reforecast data obtained from CGCMs over different regions and seasons (Jiang et al. 2013; Ogutu et al. 2017; Saha et al. 2016; Lu et al. 2017; Madrigal et al. 2018; among many others). A thorough summary of the results of these studies indicates that seasonal predictability of the key climatic variables (e.g., temperature and precipitation) over tropics is higher

as compared to the mid and high latitude regions (Dunstone et al. 2016; Ehsan et al. 2019).

Several observational and modeling studies have been conducted to investigate the impact of ENSO and other climatic drivers on winter precipitation in CSWA (Barlow et al. 2002, 2005, 2007; Barlow 2011; Hoell et al. 2015b, 2017b, 2018a, b). The ENSO signal over the CSWA has increased in recent decades (e.g., Kang et al. 2015), and some studies documented the connection between CSWA winter precipitation and its variability to ENSO (Hoell et al. 2012, 2013a, b; Hoell and Funk 2013; Rana et al. 2018; among others). Therefore, there is an opportunity to research boreal winter precipitation potential predictability and skill assessment using CGCM seasonal forecast datasets focusing over northern Pakistan, which is the dominant precipitation region in CSWA. In this study, we analyze the potential predictability and forecast skill of seasonal mean winter precipitation over NP by using retrospective ensemble seasonal forecasts obtained from six CGCMs during the period 1983–2018. The assessment is performed both with single and multimodel ensemble predictions. The article is organized as follows. Section 2 introduce the models, forecast, observational, and reanalysis datasets. It also describes the methodology used to assess the potential predictability and skill of the boreal winter NP precipitation. Observed and predicted mean and variability analysis of winter precipitation, regional precipitation connections with ENSO and atmospheric circulation, potential predictability, and skill assessment, are presented in Sect. 3. A summary and conclusions are given in Sect. 4.

2 Data and analysis method

2.1 Prediction data

Seasonal initialized Prediction data used in this work come from the North American Multimodel Ensemble (NMME) project (Kirtman et al. 2014). The NMME (see Table 1) is a forecasting system consisting of coupled models from

US and Canadian research and operational modelling centers. Real-time predictions of NMME have been started since August 2011, and there is hindcast available (forecast in the past) for each model that includes the period from 1982–2010. Here we use integration with observed November start date from the hindcast period (1982–2010) and the real-time period (2011–2018). We make no distinction between hindcast and real-time forecast in our analysis and refer to both as predictions.

The focus of the current study is to analyze the potential predictability and skill of boreal winter precipitation over northern Pakistan from initial condition observed in November (Lead-1) using individual model and multimodel ensemble (MME: a combination of six models and 79 ensemble members) approach. “Lead-1” prediction is based on Nov. initial conditions (IC), and it is the prediction for December. The prediction for Nov. itself can be considered as “Lead-0” forecast. Following this, the seasonal Lead-1 forecast is for the 3 months (December to February: DJF) following the initial month of Nov. Table 1 lists the models included in this study along with their acronym, ensemble size, native atmospheric and oceanic resolutions, prediction length and reference papers. Hindcast and real-time prediction of monthly averages of precipitation and sea surface temperature are available for download from the International Research Institute for Climate and Society (IRI) (<https://iridl.ldeo.columbia.edu/SOURCES/Models/NMME/>).

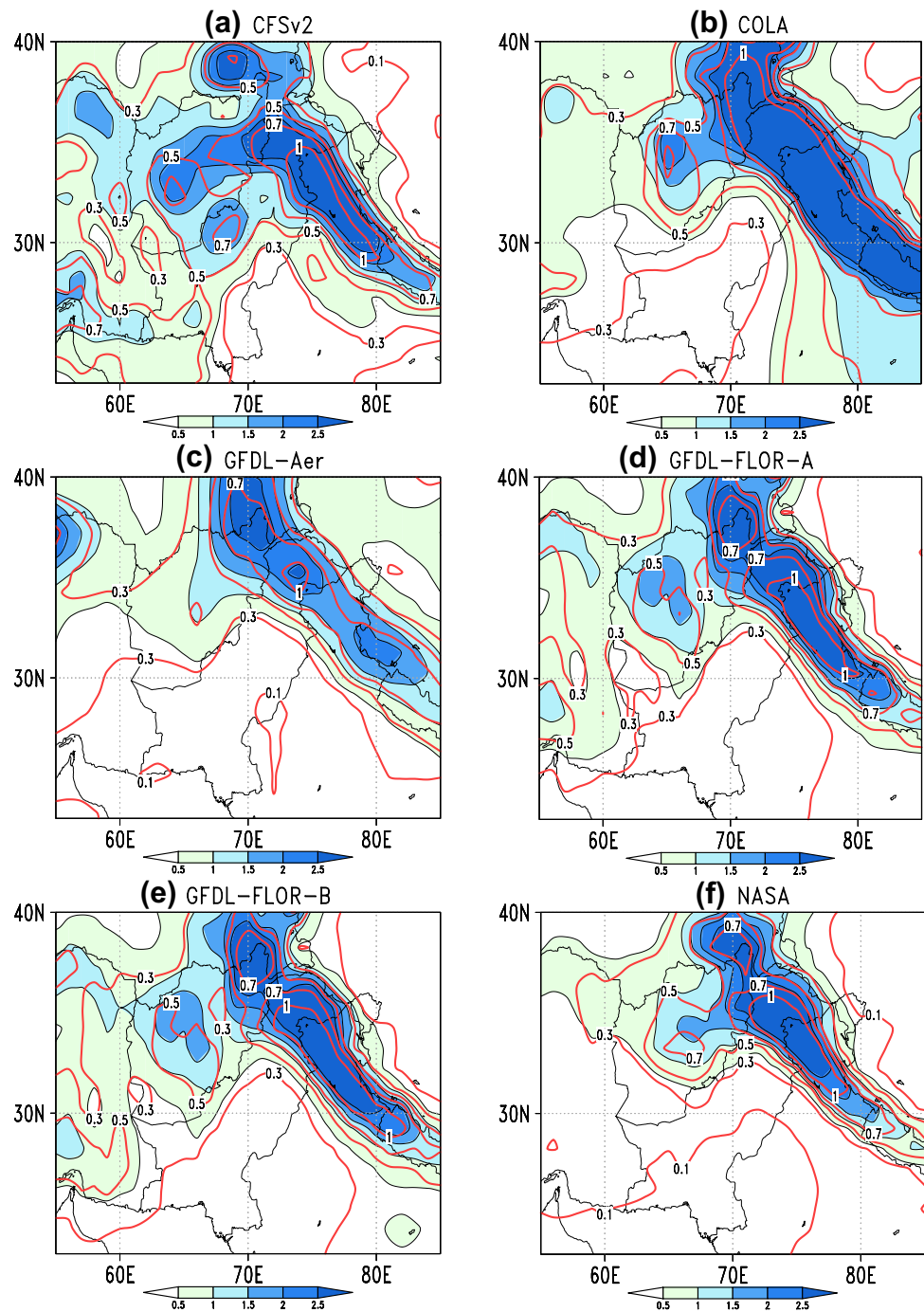
2.2 Observational data

We use several monthly mean observational and reanalysis datasets, including precipitation from the Global Precipitation Climatology Project (GPCP) version 2.3 combined precipitation dataset ($2.5^\circ \times 2.5^\circ$) (Adler et al. 2003), sea surface temperature (SST) from monthly NOAA Optimum Interpolation (OI) SST V2 ($1.0^\circ \times 1.0^\circ$) (Reynolds et al. 2002), while geopotential height is from NCEP-DOE (National Centers for Environmental Prediction-Department of Energy) AMIP-II Reanalysis products ($2.5^\circ \times 2.5^\circ$) (Kanamitsu et al. 2002). All these datasets are at different

Table 1 Six seasonal prediction models used in this work

Model	Acronym used	Ensemble members	Native atm. res.	Native ocn. res.	Prediction length (months)	References
NCEP-CFSv2	CFSv2	24	T126L64	MOM4L40 0.25° Eq.	10	Saha et al. (2014)
COLA-RSMAS-CCSM4	COLA	10	T85L261	POPL42 0.3° Eq.	12	Kirtman and Min (2009)
GFDL-CM2p1-aer04	GFDL-Aer	10	$2.0^\circ \times 2.25^\circ$ L24	MOM4L50 0.3° Eq.	12	Delworth et al. (2006)
GFDL-CM2p5-FLOR-A06	GFDL-FLOR-A	12	C18L32 (50 km)	MOM4L50 0.3° Eq.	12	Vecchi et al. (2014)
GFDL-CM2p5-FLOR-B01	GFDL-FLOR-B	12	C18L32 (50 km)	MOM4L50 0.3° Eq.	12	Vecchi et al. (2014)
NASA-GAMO-062012	NASA	11	$1.0^\circ \times 1.25^\circ$ L72	MOM4L40 0.25° Eq.	9	Vernieres et al. (2012)

Fig. 2 Predicted DJF precipitation climatology (shaded) and standard deviation (contour) calculated based on 36-year prediction data (initialized in Nov./Lead-1) for **a** CFSv2 **b** COLA **c** GFDL-Aer **d** GFDL-FLOR-A **e** GFDL-FLOR-B, and **f** NASA. Unit of precipitation is mm day^{-1}



resolutions and were converted to a $(1.0^\circ \times 1.0^\circ)$ resolution using bilinear interpolation common to prediction data.

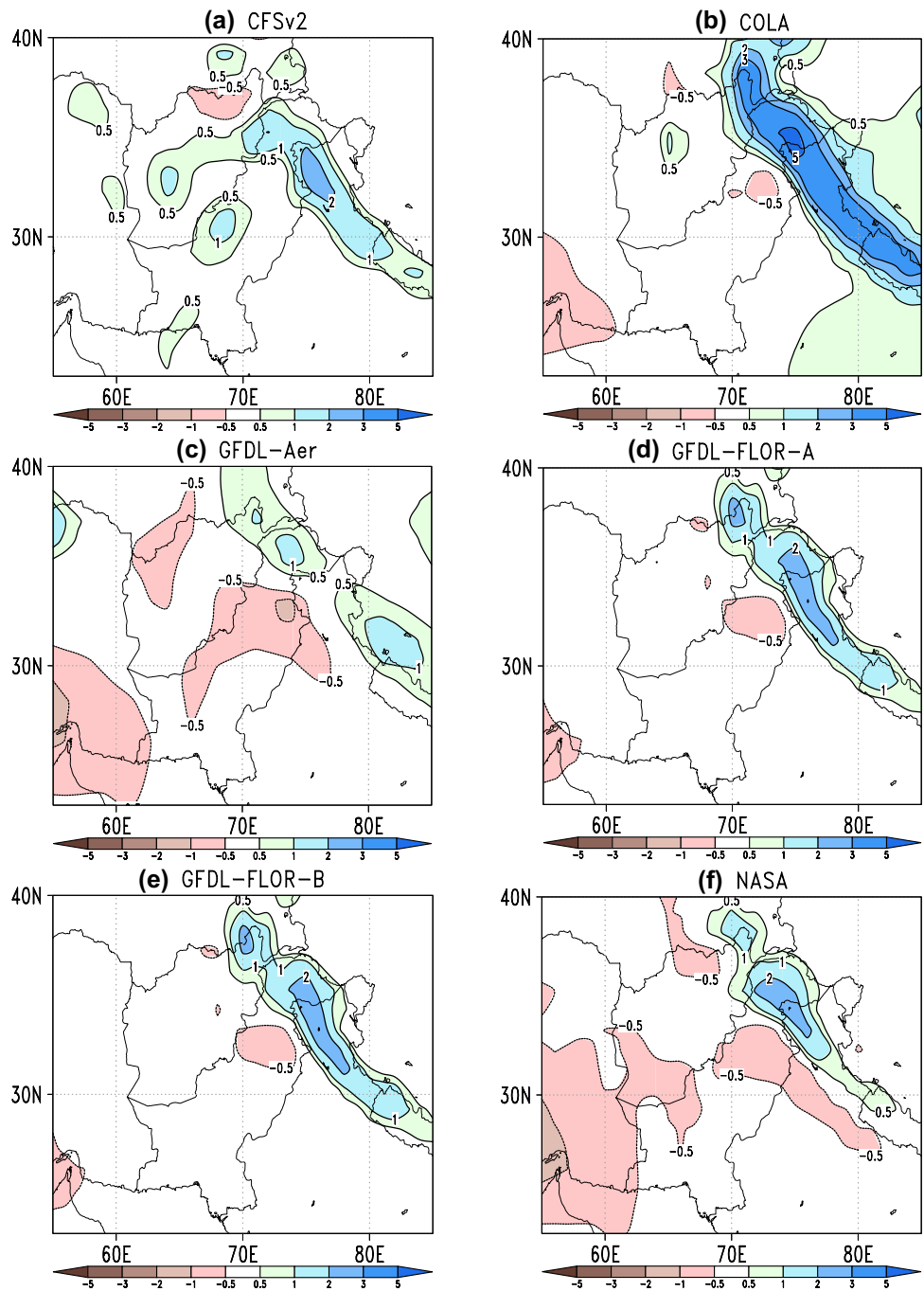
2.3 Analysis method

Seasonally averaged data for 36 boreal winters (December to February: DJF) 1982–83 to 2017–2018 is used both for observation and prediction. We define northern Pakistan domain to be all the land points included within

$68^\circ\text{--}78^\circ\text{E}$, $31^\circ\text{--}37^\circ\text{N}$. Boreal winter seasonal anomalies for each model and observation are computed relative to the 36-year climatology.

The potential predictability of boreal winter NP precipitation is assessed here as the variance of the ensemble mean also known as “Signal or external variance,” and the mean variance of ensemble deviations commonly known as “Noise or internal variance” (Rowell 1998). Following Rowell et al. (1995), signal or external variance can be expressed as;

Fig. 3 Mean DJF precipitation bias (Model-OBS) calculated based on 36-year prediction data (initialized in Nov./Lead-1) for **a** CFSv2 **(b)** COLA **(c)** GFDL-Aer **(d)** GFDL-FLOR-A **e** GFDL-FLOR-B, and **f** NASA. Unit of precipitation is mm day⁻¹



$$\sigma_{\text{Ext}}^2 = \frac{1}{N-1} \sum_{k=1}^N \left(\bar{P}_k - \bar{\bar{P}} \right)^2,$$

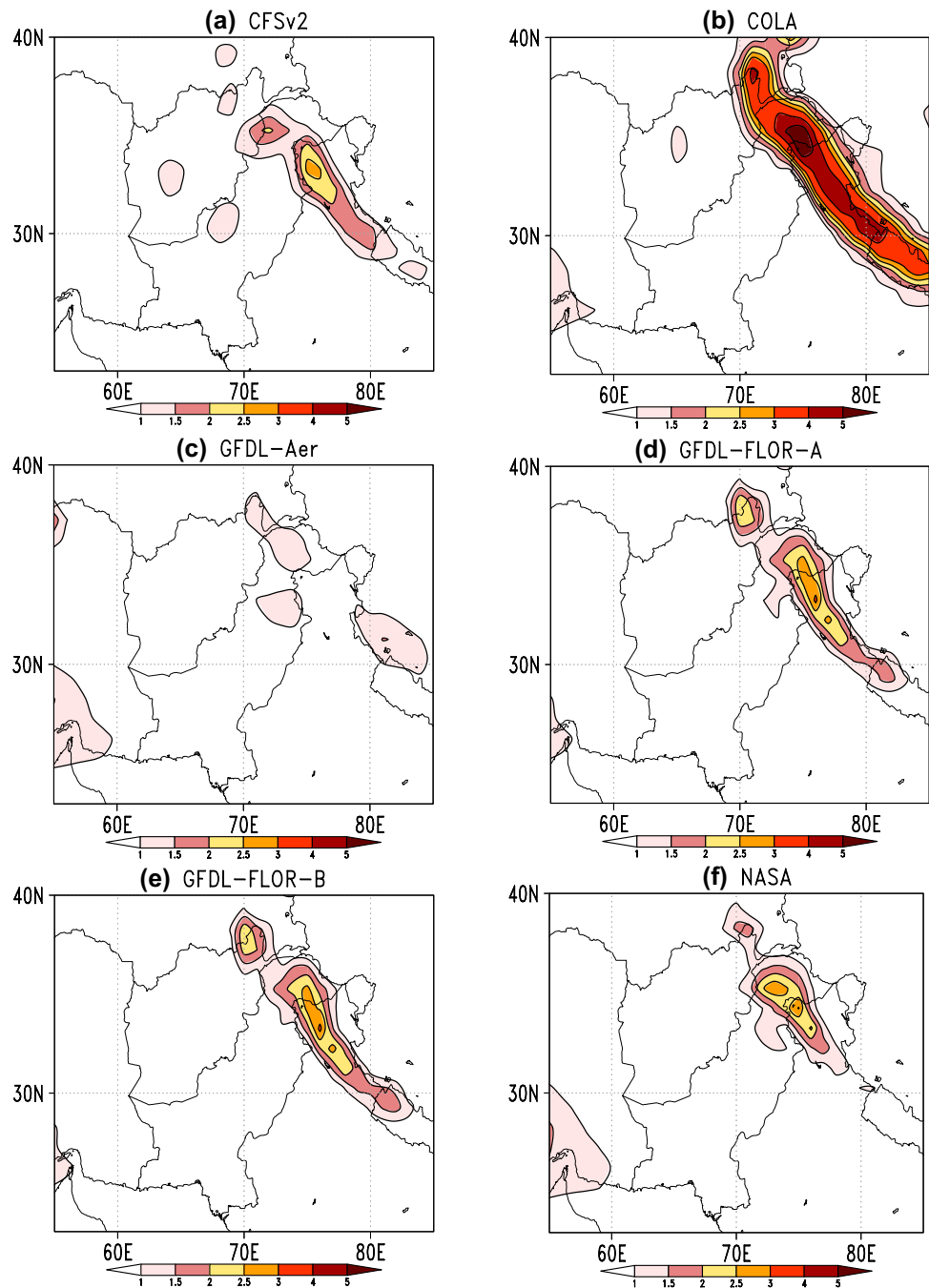
where P is the precipitation, $\bar{\bar{P}}$ is the climatological mean of the ensemble mean given by $\bar{\bar{P}} = \frac{1}{Nn} \sum_{k=1}^N \sum_{m=1}^n P_{km}$ and \bar{P}_k is the ensemble mean. Here k indicates the specific year and m denotes ensemble members. The noise or internal variance can be expressed as;

$$\sigma_{\text{Int}}^2 = \frac{1}{N(n-1)} \sum_{k=1}^N \sum_{m=1}^n (P_{km} - \bar{P}_k)^2,$$

The ratio of signal and noise variances (S/N Ratio) defines potential predictability (Kang and Shukla 2006).

$$\text{S/N Ratio} = \frac{\sigma_{\text{Ext}}^2}{\sigma_{\text{Int}}^2},$$

Fig. 4 Same as Fig. 3, but for root-mean-square-error (RMSE). Unit of precipitation RMSE is mm day^{-1}



The potential skill is estimated by using the perfect model correlation (PMC) method, which is calculated as the “correlation between ensemble average and one ensemble member” and provides the predictive skill of that ensemble member (Ehsan et al. 2013). Following ‘m’ ensemble members ‘m’ correlations are averaged by using Fisher Z transformation. The prediction skill of boreal winter NP precipitation is assessed here is through the computation of the temporal anomaly correlation coefficient (TCC) between the ensemble mean and observed time series. The student t test is used to calculate the

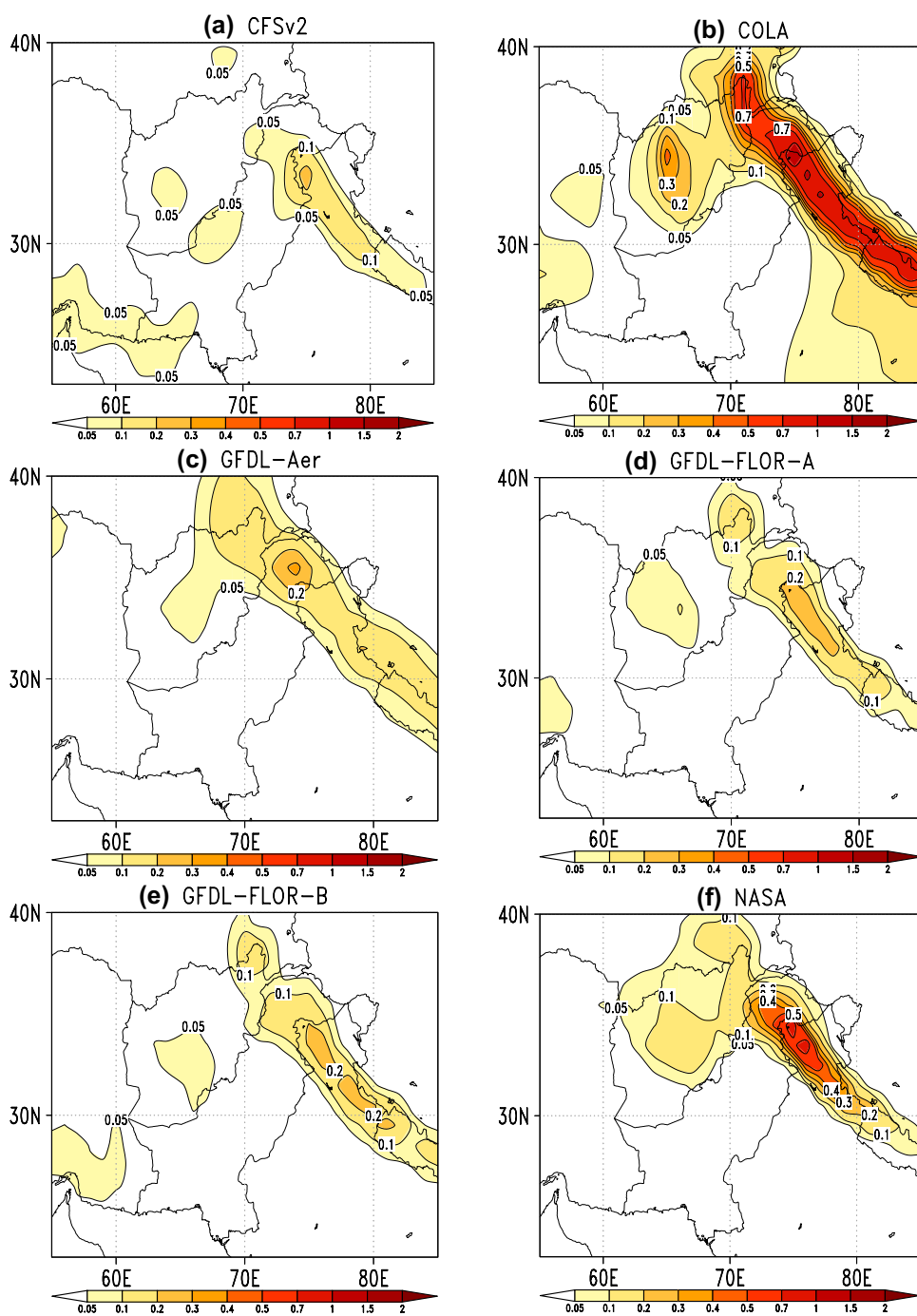
statistical significance of the correlation (Wilks 2006), by considering a threshold value of 0.05.

3 Results

3.1 Observed and predicted mean and variability

The climatological mean DJF precipitation (shaded) and standard deviation (contour) obtained from the gridded GPCP dataset averaged over the period 1983–2018 is

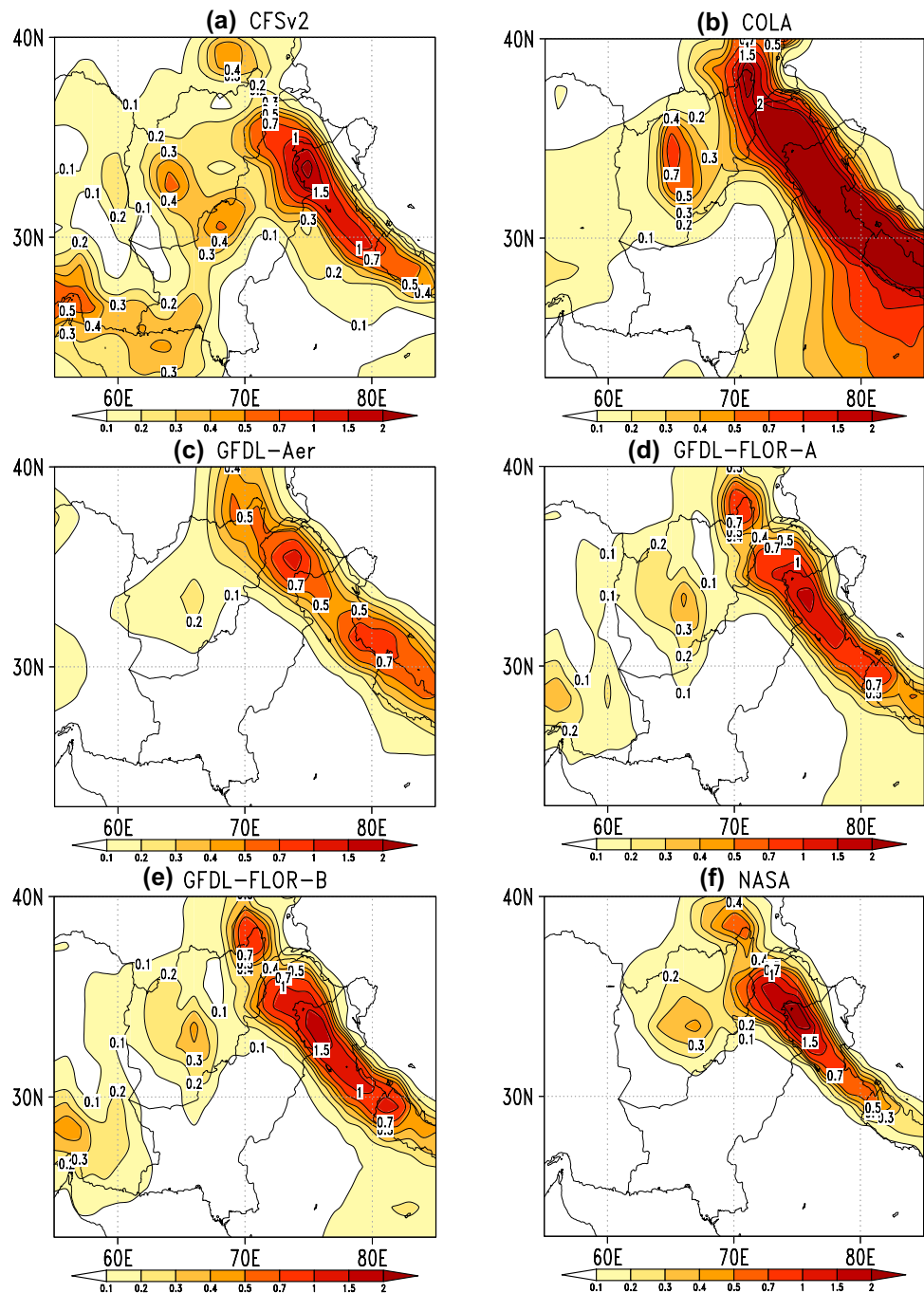
Fig. 5 Signal variance of DJF precipitation estimated based on 36-year prediction data (initialized in Nov./Lead-1) for **a** CFSv2 **b** COLA **c** GFDL-Aer **d** GFDL-FLOR-A **e** GFDL-FLOR-B, and **f** NASA. Unit of signal variance is $\text{mm}^2 \text{day}^{-2}$



shown in Fig. 1b. The spatially averaged winter precipitation over NP estimated from observation is 1.38 mm day^{-1} with a standard deviation of 0.50 mm day^{-1} . The coefficient of variation is 37%, which shows that year-to-year precipitation variability is quite high as compared to the mean winter precipitation. The sizeable interannual variability is evident in spatially averaged winter precipitation time series (Fig. 1c). The geographical distribution

of correlation between spatially averaged winter Precipitation time series and gridded precipitation for 36 years is shown in Fig. 1d. The NP precipitation is highly positively correlated over the whole NP region and shows positive covariability with contiguous northeast Afghanistan and northwest Indian regions. Moreover, the NP precipitation during DJF shows episodes (Fig. 1c) of below average precipitation during 1999–2002, which coincide with the

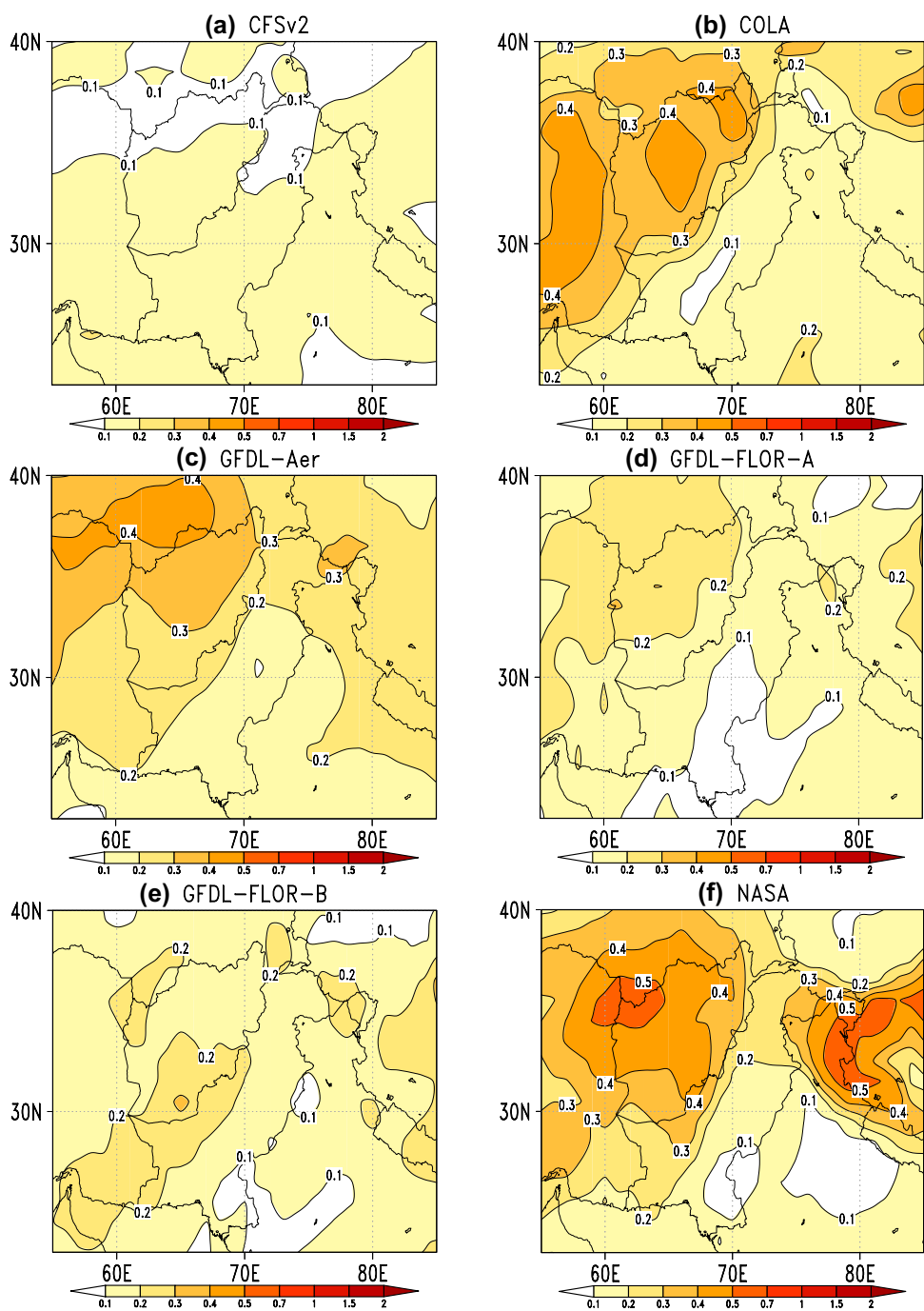
Fig. 6 Same as Fig. 5, but for noise variance. Unit of noise variance is $\text{mm}^2 \text{day}^{-2}$



consecutive four drought years of CSWA in recent decades (Barlow et al. 2002, 2016). Socioeconomic impacts of this drought period were severe over the region (Agrawala et al. 2001), with shortened water availability resulting in reduced agriculture production and livestock populations that result in rural-to-urban population migration and also ignite unrest among local communities (Ali et al. 2018; Batool and Saeed 2018).

Before analyzing the potential predictability and skill of boreal winter NP precipitation, it is desirable to first assess the fidelity of individual models in comparison to observation. The spatial structure of predicted boreal winter precipitation climatology (shaded) and interannual variability represented by the standard deviation (contour) for the period 1983–2018 is shown in Fig. 2. Individual models well simulate the geographical distribution of mean and

Fig. 7 Signal-to-noise ratio (S/N Ratio) of DJF precipitation estimated based on 36-year prediction data (initialized in Nov./Lead-1) for **a** CFSv2 **b** COLA **c** GFDL-Aer **d** GFDL-FLOR-A **e** GFDL-FLOR-B, and **f** NASA. S/N Ratio is unitless



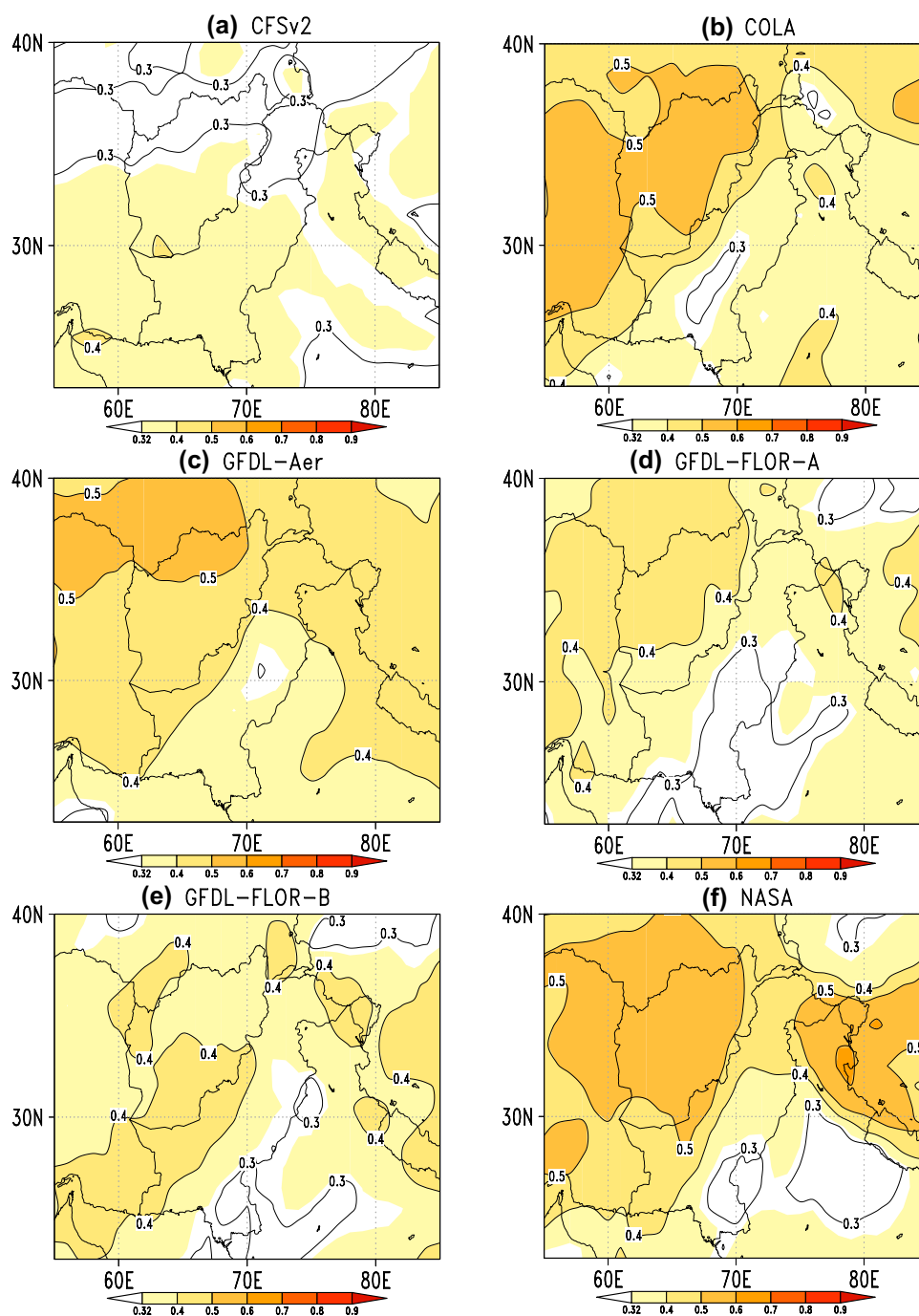
variability of boreal winter precipitation as compared to observation. However, all models strongly overestimated both mean and variability (based on individual model realizations) over the region of interest. The difference (Model-Observed) between predicted and observed climatological seasonal mean DJF precipitation is shown in Fig. 3. All models show wet bias over the NP, particularly over the foothills of the Himalayas. For each model, we also calculate the root-mean-square-error against the observed DJF precipitation measurements (Fig. 4). The

COLA (GFDL-Aer) models (Fig. 4b, c) show the highest (lowest) RMSE as compared to other models.

3.2 Winter NP precipitation predictability assessment

The geographical distributions of signal, noise, and signal-to-noise ratio (S/N Ratio) are elucidated in Figs. 5, 6, and 7, respectively. Spatial distribution and magnitude of signal and noise variances vary by model. Signal variance is quite

Fig. 8 Potential skill of DJF precipitation estimated using perfect model correlation which is based on 36-year prediction data (initialized in Nov./Lead-1) for **a** CFSv2 **b** COLA **c** GFDL-Aer **d** GFDL-FLOR-A **e** GFDL-FLOR-B, and **f** NASA. A correlation coefficient higher than 0.32 is statistically significant at 5% confidence level, using a *t* test

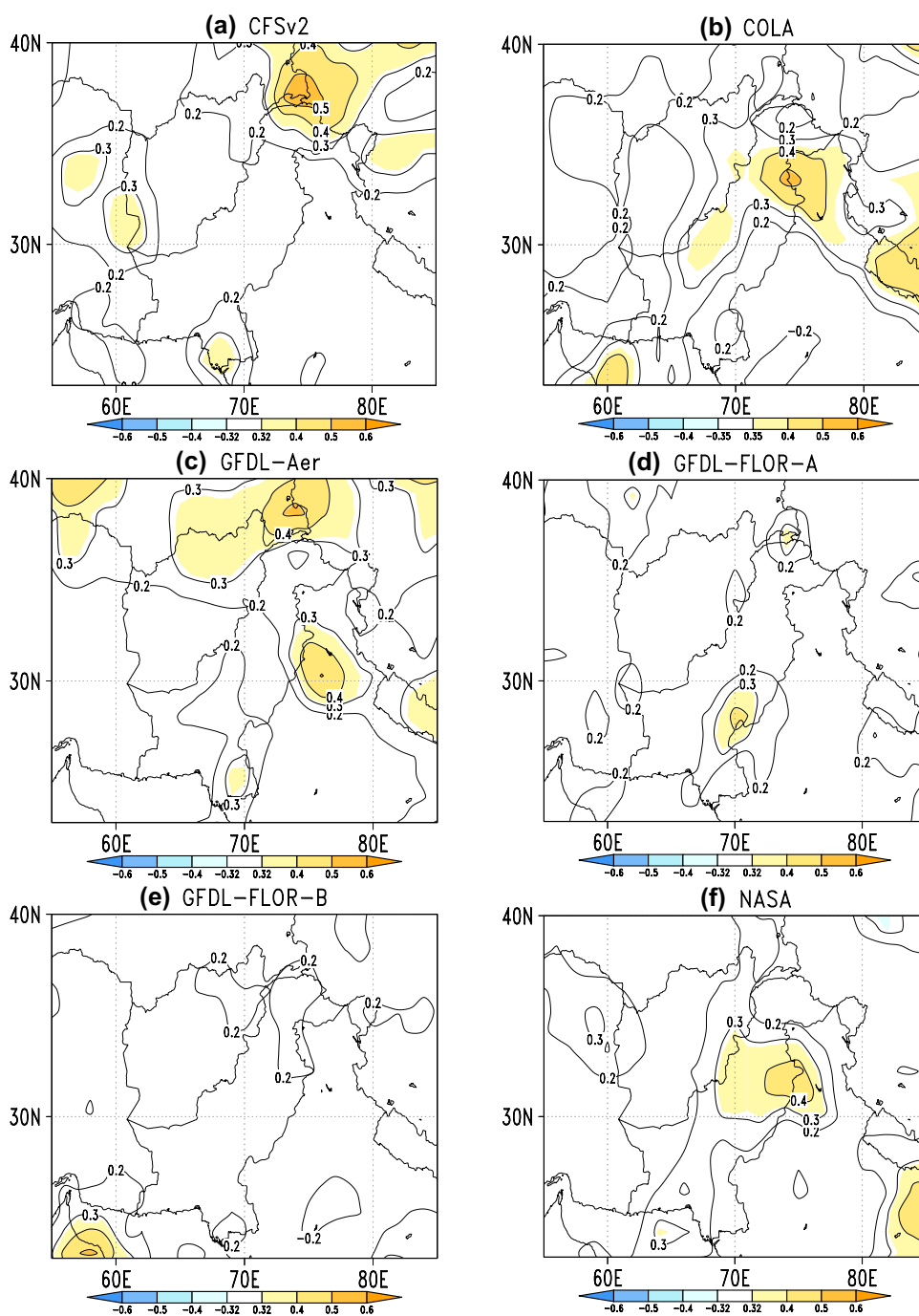


weak (Fig. 5) as compared to noise variance, which shows quite high values in all models (Fig. 6). Northern Pakistan region shows high signal variance, while noise variance is even larger and almost uniformly distributed over the whole region. COLA model shows large signal variance (Fig. 5b), but it also tends to have even larger noise variance (Fig. 6b). The regions with high (low) signal-to-noise ratio tend to have a higher (lower) potential predictability (Fig. 7). The S/N Ratio ≥ 1.84 (1.60) is considered as significant at 95

(90) % level based on F-ratio statistics. Due to substantially high values of internal atmospheric variability, the signal-to-noise ratio tends to show quite low values in all models (Fig. 7), which shows an inherent low potential predictability over the region of interest. However, NASA model (Fig. 7f) shows highest S/N Ratio as compared to other models.

The spatial distribution of perfect model correlation (ensemble member against ensemble mean) is shown in Fig. 8. PMC is an indication of the upper limit of the

Fig. 9 Prediction skill (correlation between ensemble mean and observed anomalies) of DJF precipitation based on 36-year prediction data (initialized in Nov./Lead-1) for **a** CFSv2 **b** COLA **c** GFDL-Aer **d** GFDL-FLOR-A **e** GFDL-FLOR-B, and **f** NASA. A correlation coefficient higher than 0.32 is statistically significant at 5% confidence level, using a *t* test



dynamical seasonal prediction skill that can be achieved with a perfect model and perfect boundary conditions. The figure indicates that the potential predictability of the boreal winter NP precipitation is relatively low. The COLA, GFDL-Aer, and NASA models (Fig. 8b, c, f) show moderate but statistically significant potential skill over the region of interest, while all other models (CFSv2, GFDL-FLOR-A, and GFDL-FLOR-B) depict quite low values of PMC over the region of

interest. The spatial distribution of prediction skill for boreal winter NP precipitation in terms of TCC (ensemble mean correlated with observation) is shown in Fig. 9. Statistically significant TCC values are observed over the northern latitudes (adjoining areas of Afghanistan, Pakistan, and Tajikistan) in CFSv2 (Fig. 9a) and GFDL-Aer (Fig. 9c), while no significant values are witnessed over the region of interest. However, COLA (Fig. 9b) and NASA (Fig. 9f) models show

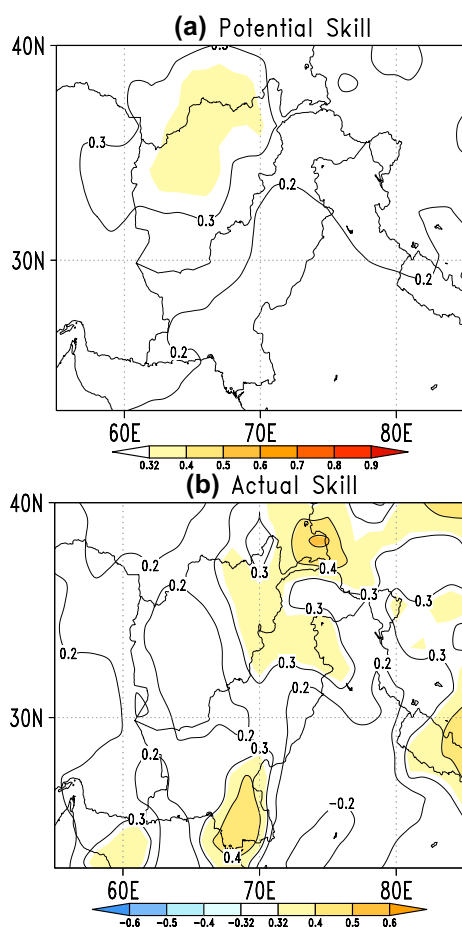


Fig. 10 **a** Potential and **b** actual skill estimated based on 36-year prediction data (initialized in Nov./Lead-1) for MME (six models and 79 members). A correlation coefficient higher than 0.32 is statistically significant at 5% confidence level, using a t test

reasonable statistically significant skill over the NP region. The two GFDL models (FLOR-A and FLOR-B) show the lowest actual skill (Fig. 9d, e). Recently, Cash et al. (2017) demonstrated that individual models and multimodel ensemble of NMME are less skillful in predicting precipitation and temperature at different leads over Pakistan-Afghanistan (60° – 75° E, 23° – 39° N) as compared to Extended Indian Monsoon Rainfall region (70° – 100° E, 10° – 30° N) due to the complex mountainous terrain of the former. They attributed this low skill to the relatively low resolution of the simulations that are not able to resolve the complex topography of the region in these models (Cash et al. 2017).

Turning our attention to the multimodel ensemble, we now reveal the potential predictability and skill of the multimodel ensemble (a combination of six models and 79

ensemble members) in predicting boreal winter precipitation over the CSWA region. Several earlier (e.g., Palmer et al. 2004; Hagedorn et al. 2005) studies have confirmed the superiority of multimodel ensemble predictions over that of a single model. We show the spatial distribution of potential and actual skills of boreal winter precipitation over CSWA (Fig. 10). MME based potential skill (Fig. 10a) clearly shows the underperformance of MME as compared to the individual models (Fig. 8). Figure 10b shows the spatial distribution of actual prediction skill for winter NP precipitation based on MME. In contrast to PMC, MME shows quite high values (statistically significant) of TCC over the NP domain, which is an indication of underconfident forecasts (Eade et al. 2014) in which ensemble members do not agree well with each other (low PMC) but do capture the observed variations quite well (high TCC).

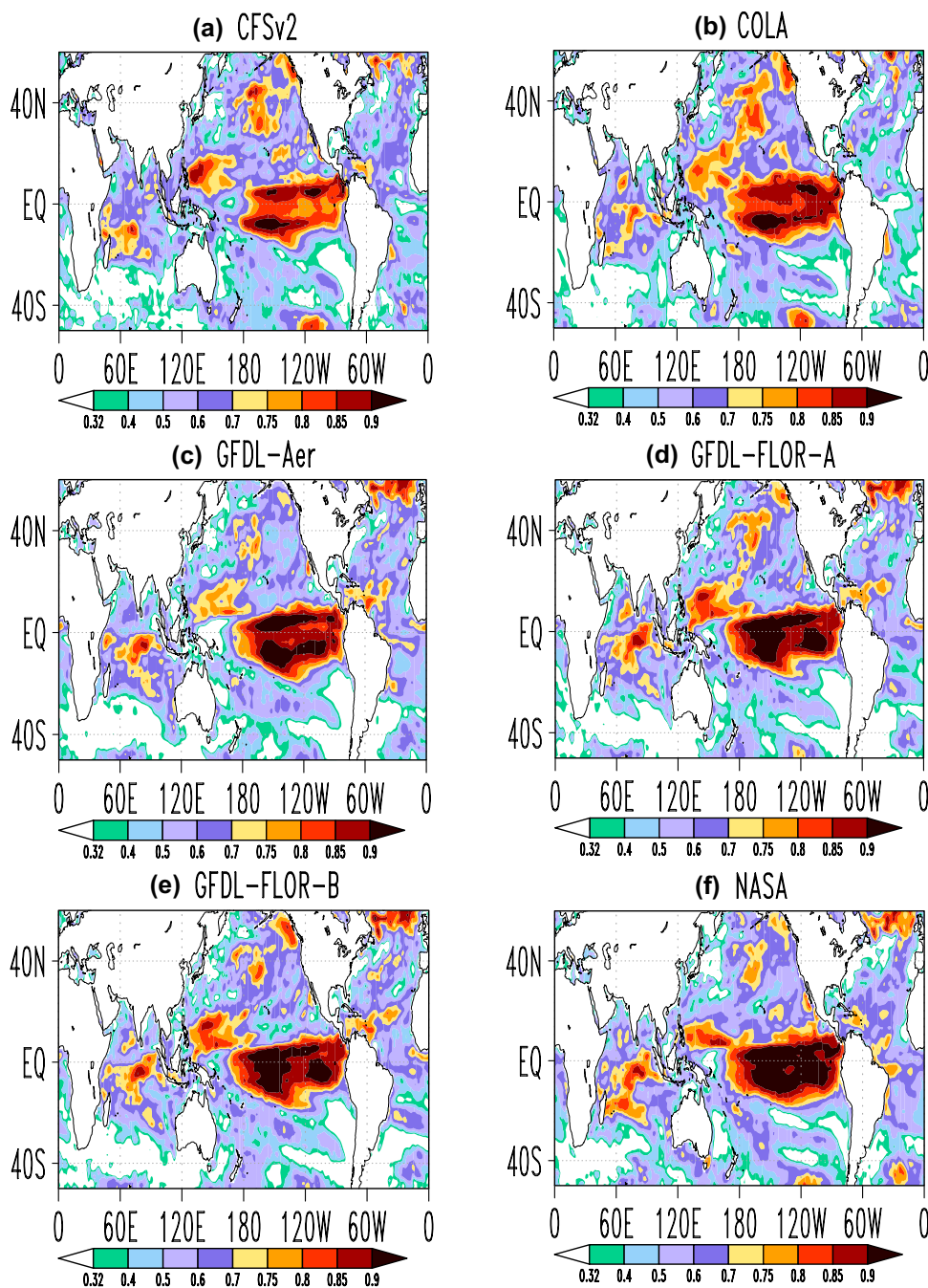
3.3 SST prediction skill and observed and predicted teleconnections

In the previous section, we have seen a significant difference in predicting potential and real skill of boreal winter CSWA precipitation in initialized models. Two main questions will be answered in this section: (1) do the models (e.g., COLA and NASA) that have higher CSWA precipitation skill also make a better SST forecast as compared to other models? (2) how well these models that show higher precipitation skill predict the boreal winter precipitation teleconnection with SSTs and atmospheric circulation as compared to observation and other models?

Figure 11 shows the global spatial distribution of the correlation coefficient between the observed and predicted ensemble mean DJF SSTs anomalies for each model. As elucidated in the introduction, the interannual and intra-seasonal variability of winter precipitation over CSWA is strongly influenced by SST variability over the Pacific and Indian Oceans. Thus, simulation of SST and the teleconnection with winter NP precipitation are critical for an accurate representation of seasonal mean winter precipitation and its predictability in initialized models. The figure indicates that the SST prediction skill is relatively high in the tropical oceans, particularly in the tropical (western, central, eastern) Pacific, and the tropical Indian Ocean. There is a considerably higher SST prediction skill in the NASA model (Fig. 11f) as compared to other models.

Now we identify the relationship between winter NP precipitation and global SSTs and upper-level geopotential height (Z200) in observation, and their reproduction in

Fig. 11 Prediction skill (correlation between ensemble mean and observed anomalies) of DJF SST based on 36-year prediction data (initialized in Nov./Lead-1) for **a** CFSv2 **b** COLA **c** GFDL-Aer **d** GFDL-FLOR-A **e** GFDL-FLOR-B, and **f** NASA. A correlation coefficient higher than 0.32 is statistically significant at 5% confidence level, using a *t* test



prediction data. Figure 12a shows the distribution of spatial correlation between spatially averaged DJF precipitation over NP and SST anomalies for the period 1983–2018. The DJF NP precipitation is positively correlated over the central-eastern equatorial Pacific as well as the tropical Indian Ocean and the Arabian Sea. The positive correlation coefficient in the ENSO region shows that the ENSO tends to boost (suppress) winter precipitation in the region during warm (cold) events (Hoell et al. 2014; Rana et al.

2017). Warmer than average SST anomalies in ENSO region develops deep convection, releasing latent heat in a deep atmospheric column and producing an upper-level divergence in the central-eastern Pacific, which is balanced to a first order by descending motion and upper-level convergence in the western Pacific in boreal winter. This upper-level convergence in the western Pacific acts as a source for tropical cyclonic upper-level Rossby gyre further to the west in the CSWA region through syerdrup balance mechanism.

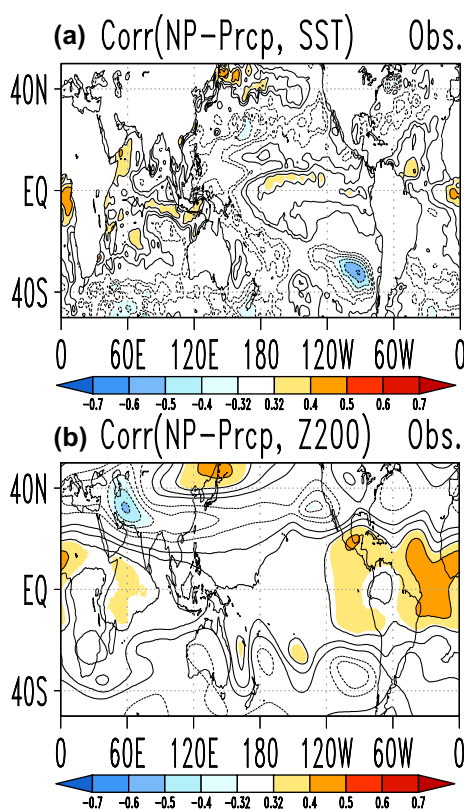


Fig. 12 The correlation of DJF precipitation anomalies (spatially averaged over NP domain) with **a** global sea surface temperature and **b** 200 hPa geopotential height (Z200). The data period is from 1983–2018. A correlation coefficient higher than 0.32 is statistically significant at 5% confidence level, using a *t* test

The correlation maps between spatially averaged DJF NP precipitation and Z200 circulation anomalies is shown in Fig. 12b. A statistically significant positive correlation is observed over the tropical areas, and negative correlation appears over the subtropical Asia (20° to 40° northern latitudes) extending from the Middle East to western Pacific for Z200 (Fig. 12b). The negative correlation indicates that the winter precipitation anomalies in the region are associated with the upper-level cyclonic circulation anomalies over the region.

We expect that capturing the appropriate teleconnection pattern in prediction data is essential for better prediction skill. In order to have a fair comparison, the spatially averaged precipitation over NP for a particular model is calculated for each ensemble separately and correlated with the SST global field of that ensemble member. This is done for each of the *m* ensemble members, and the *m* correlations are averaged, after applying Fisher Z transformation (Ehsan et al. 2017a). Each model captures the observed relationship between spatially averaged DJF precipitation over NP, with sea surface temperature with varying details. Compared with observations, the SST-precipitation link is reasonably

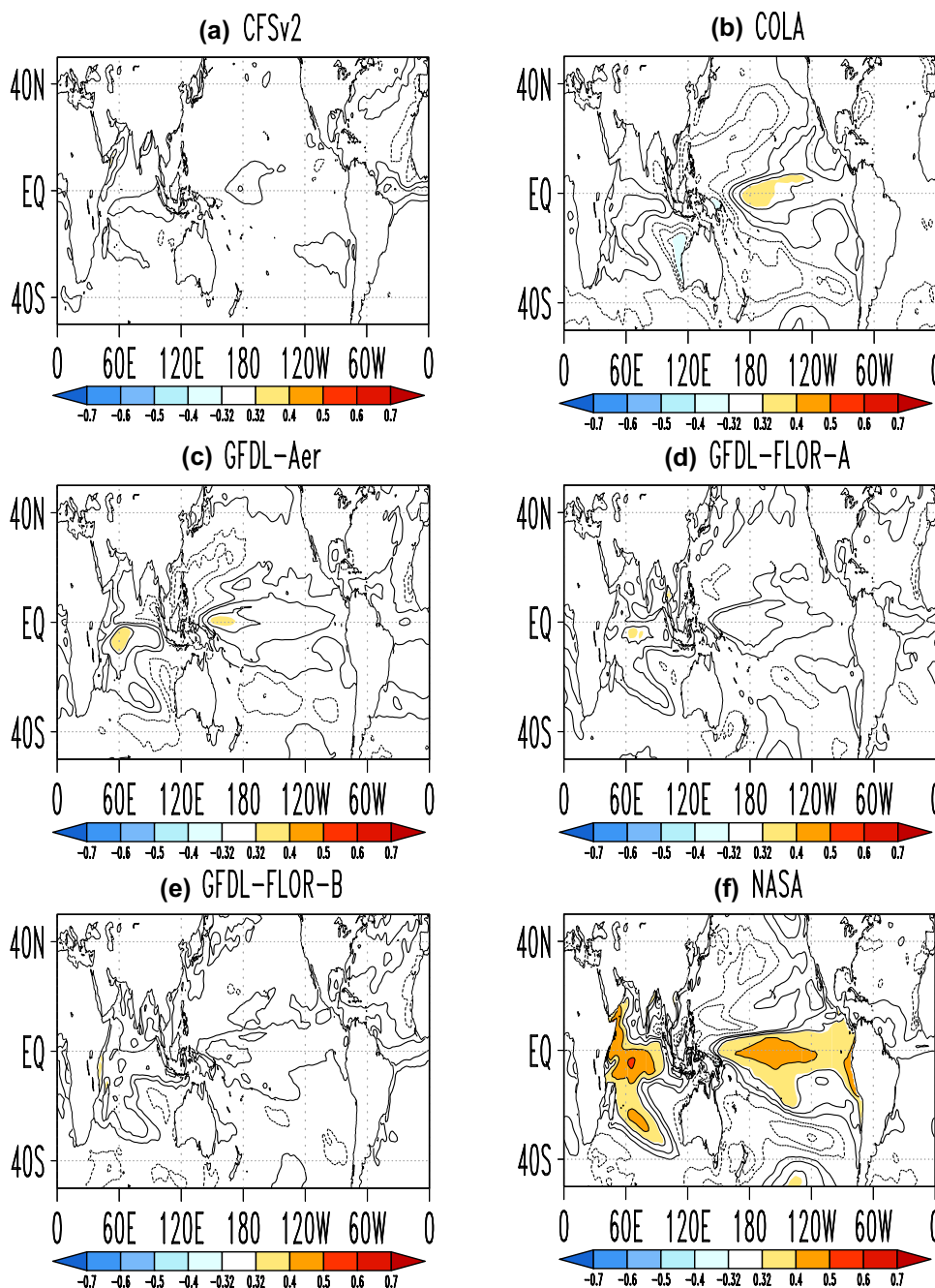
reproduced in COLA and NASA models (Fig. 13b, f) as compared to other models. However, the teleconnection pattern is slightly stronger as compared to the observed pattern in NASA model (Fig. 13f). The outperformance of these models is also evident in the DJF NP-Precipitation-Z200 analysis, which shows negative correlation over the CSWA region and positive values in the tropical regions (Fig. 14f) statistically significant at 95% level. This indicates that the predicted teleconnection pattern in these models is quite well reproduced as compared to the observed pattern, which may have a positive impact on the winter NP precipitation predictability in these models. Other models are also able to capture the negative (positive) correlation over the CSWA (tropical) region with varying details. However, the teleconnection patterns predicted in these models poorly matched the observation (statistically insignificant), indicating that more attention is needed on the tropical/extratropical teleconnection patterns in initialized models.

4 Summary and conclusions

The potential predictability intrinsically depends on the model characteristics. In other words, different models produce different signal and noise combinations and, therefore, different potential predictability is represented by the signal-to-noise ratio. The potential predictability and skill of precipitation over CSWA during boreal winter is investigated in the present study. The assessment focused over the northern Pakistan where observed winter precipitation is a substantial fraction of the annual total, and this region stands out as receiving substantial winter precipitation in central-southwest Asia. The prediction datasets at Lead-1 (based on Nov. observed initial conditions) is utilized in the present study come from a subset of the North American Multimodel Ensemble during the period 1983–2018 (six models and 79 ensemble members). The main findings from this study are summarized below.

- Initialized models capture the observed mean features including; climatological mean DJF precipitation and variability over the region. However, some systematic biases/errors in the prediction of the winter climatological mean precipitation are also observed, e.g., overestimation of precipitation over the foothills of the Himalayas.
- The potential and actual prediction skills of winter CSWA precipitation are low because the potentially predictable component (signal) is small as compared to the unpredictable quantity (noise).
- Each model, with varying details, captures observed teleconnection patterns. However, the COLA and NASA models reasonably reproduced these teleconnection pat-

Fig. 13 The correlation of DJF NP precipitation anomalies (spatially averaged over NP domain) with SST anomalies for **a** CFSv2 **b** COLA **c** GFDL-Aer **d** GFDL-FLOR-A **e** GFDL-FLOR-B, and **f** NASA. A correlation coefficient higher than 0.32 is statistically significant at 5% confidence level, using a *t* test. The correlation is computed within each ensemble member separately and then average for all ensemble members (see text for details)



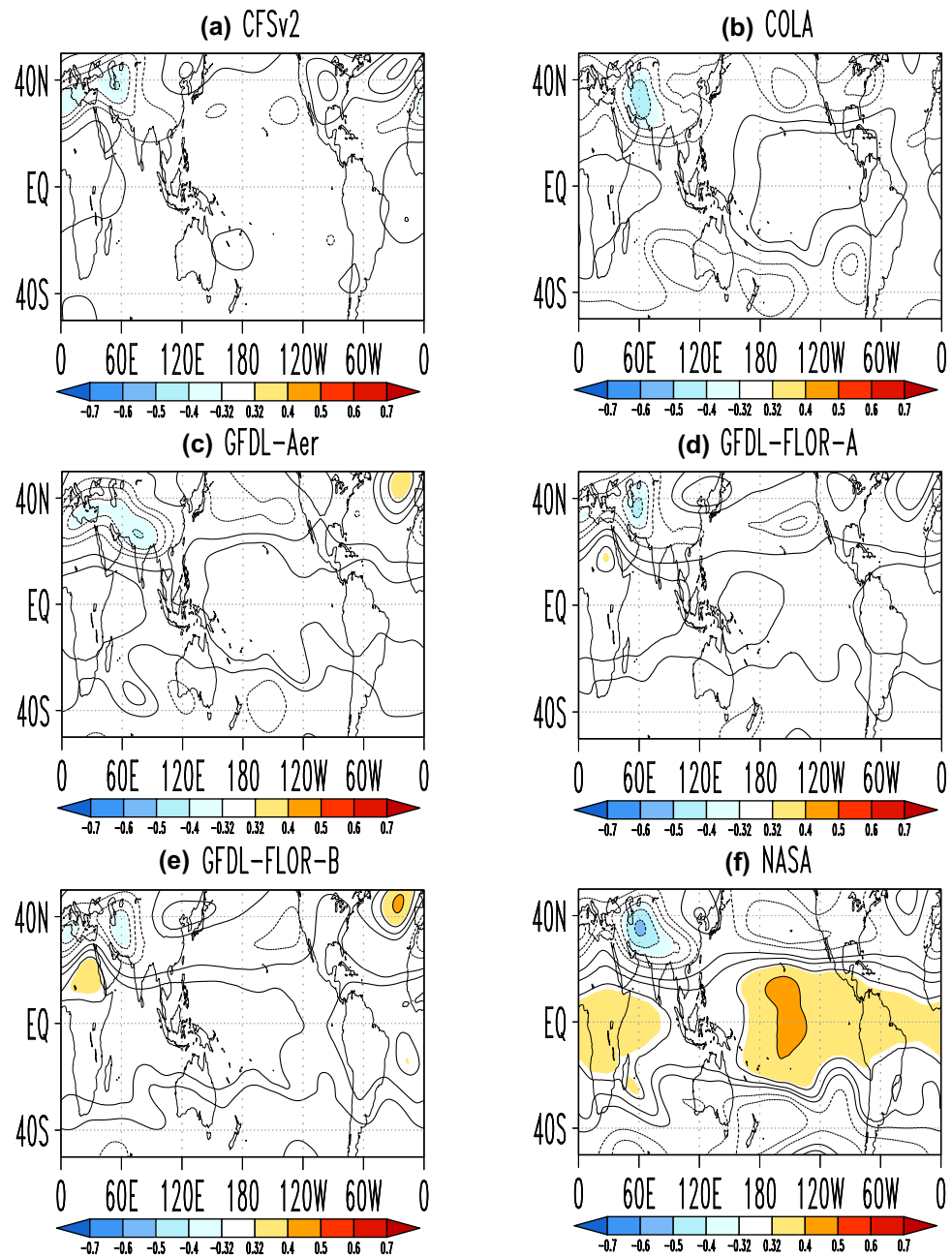
terns as compared to other models. It also found that SSTs in the tropical Oceans are relatively well predicted by NASA model when compared with other models.

- Use of MME shows an underperformance in estimating potential and actual skill over the region of interest as compared to individual models.

This study reveals the inadequate performance of current state-of-the-art seasonal prediction models in predicting

winter precipitation over northern Pakistan. Better representation of the teleconnection patterns in prediction data might be expected to lead to increased regional, seasonal climate predictability. Together, these results indicate that reliable prediction of the boreal winter precipitation over CSWA remains a great challenge in initialized models.

Fig. 14 Same as Fig. 13, but for Z200



Acknowledgements We are grateful to the two anonymous reviewers whose comments significantly improved the quality of the manuscript. We acknowledge NOAA MAPP, NSF, NASA, and the DOE that support the NMME-Phase II system, and we thank the climate modeling groups (Environment Canada, NASA, NCAR, NOAA/GFDL, NOAA/NCEP, and University of Miami) for producing and making available their model output. NOAA/NCEP, NOAA/CTB, and NOAA/CPO jointly provided coordinating support and led the development of the NMME-Phase II system. We also acknowledge King Abdulaziz University's High-Performance Computing Center (Aziz Supercomputer: <http://hpc.kau.edu.sa>) for providing computation support for this work.

References

- Adler RF et al (2003) The version 2 global precipitation climatology project (GPCP) monthly precipitation analysis (1979-present). *J Hydrometeorol* 4:1147–1167
- Adnan S, Ullah K, Gao S, Khosa AH, Wang Z (2017) Shifting of agro-climatic zones, their drought vulnerability, and precipitation and temperature trends in Pakistan. *Int J Climatol*. <https://doi.org/10.1002/joc.5019>
- Agrawala S, Barlow M, Cullen H, Lyon B (2001) The drought and humanitarian crisis in Central and Southwest Asia: a climate

- perspective. IRI Special Rep. 01-11 International Research Institute for Climate and Society, 24 pp
- Ali F, Khan TA, Alamgir A, Khan MA (2018) Climate change-induced conflicts in Pakistan: from national to individual level. *Earth Syst Environ* 2:573–599. <https://doi.org/10.1007/s41748-018-0080-8>
- Almazroui et al (2017) Saudi-KAU coupled global climate model: description and performance. *Earth Syst Environ* 1:7. <https://doi.org/10.1007/s41748-017-0009-7>
- Arnal L, Wood AW, Stephens E, Cloke HL, Pappenberger F (2017) An efficient approach for estimating stream flow forecast skill elasticity. *J Hydrometeorol* 18:1715–1729. <https://doi.org/10.1175/JHM-D-16-0259.1>
- Barlow M (2011) The Madden–Julian oscillation influence on Africa and west Asia. In: Lau W, Waliser D (eds) *Intraseasonal variability in the coupled tropical ocean-atmosphere system*. Praxis, Banagalore, pp 477–493
- Barlow M, Cullen H, Lyon B (2002) Drought in central and southwest Asia: La Niña, the warm pool, and Indian Ocean precipitation. *J Clim* 15:697–700
- Barlow M, Wheeler M, Lyon B, Cullen H (2005) Modulation of daily precipitation over southwest Asia by the Madden–Julian oscillation. *Mon Weather Rev* 133:3579–3594. <https://doi.org/10.1175/MWR3026.1>
- Barlow M, Hoell A, Colby F (2007) Examining the wintertime response to tropical convection over the Indian Ocean by modifying convective heating in a full atmospheric model. *Geophys Res Lett* 34:L19702. <https://doi.org/10.1029/2007GL030043>
- Barlow M, Zaitchik B, Paz S, Black E, Evans J, Hoell A (2016) A review of drought in the middle east and Southwest Asia. *J Clim* 29:8547–8574
- Barnston AG, Tippett MK (2013) Predictions of Nino3.4 SST in CFSv1 and CFSv2: a diagnostic comparison. *Clim Dyn* 41:1615–1633
- Batool S, Saeed F (2018) Unpacking climate impacts and vulnerabilities of cotton farmers in Pakistan: a Case study of two semi-arid districts. *Earth Syst Environ* 2:499–514. <https://doi.org/10.1007/s41748-018-0068-4>
- Cannon F, Carvalho LMV, Jones C, Hoell A, Norris J, Kiladis GN, Tahir AA (2016) The influence of tropical forcing on extreme winter precipitation in the western Himalaya. *Clim Dyn* 48:1213–1232
- Cash BA, Manganello JV, Kinter JL (2017) Evaluation of NMME temperature and precipitation bias and forecast skill for South Asia. *Clim Dyn*. <https://doi.org/10.1007/s00382-017-3841-4>
- Clark RT, Bett PE, Thornton HE, Scaife AA (2017) Skillful seasonal predictions for the European energy industry. *Environ Res Lett* 12:024002. <https://doi.org/10.1088/1748-9326/aa57ab>
- Delworth et al (2006) GFDL's CM2 global coupled climate models. Part I: formulation and simulation characteristics. *J Clim* 19:643
- Dunstone N, Smith D, Scaife A, Hermanson L, Eade R, Robinson N, Andrews M, Knight J (2016) Skillful predictions of the winter North Atlantic Oscillation one year ahead. *Nat Geosci* 9:809–814
- Eade R, Smith D, Scaife A, Wallace E, Dunstone N, Hermanson L, Robinson N (2014) Do seasonal-to-decadal climate predictions underestimate the predictability of the real world? *Geophys Res Lett* 41:5620–5628. <https://doi.org/10.1002/2014GL061146>
- Ehsan MA et al (2013) A quantitative assessment of changes in seasonal potential predictability for the twentieth century. *Clim Dyn* 41:2697–2709
- Ehsan MA, Tippett MK, Almazroui M, Ismail M, Yousef A, Kucharski F, Omar M, Hussein M, Alkhalaf AA (2017a) Skill and predictability in multimodel ensemble forecasts for Northern Hemisphere regions with dominant winter precipitation. *Clim Dyn* 48(9–10):3309–3324
- Ehsan MA et al (2017b) Sensitivity of AGCM simulated regional summer precipitation to different convective parameterizations. *Int J Climatol*. <https://doi.org/10.1002/joc.5108>
- Ehsan MA, Kucharski F, Almazroui M, Ismail M, Tippett MK (2019) Potential predictability of Arabian Peninsula summer surface air temperature in the North American multimodel ensemble. *Clim Dyn*. <https://doi.org/10.1007/s00382-019-04784-3>
- Hagedorn R, Doblas-Reyes FJ, Palmer TN (2005) The rationale behind the success of multimodel ensembles in seasonal forecasting. Part I: Basic concept. *Tellus A* 57:219–233
- Hoell A, Funk C (2013) The ENSO-related west pacific sea surface temperature gradient. *J Clim* 26:9545–9562
- Hoell A, Barlow M, Saini R (2012) The leading pattern of intraseasonal and interannual Indian Ocean precipitation variability and its relationship with Asian circulation during the boreal cold season. *J Clim* 25:7509–7526
- Hoell A, Funk C, Barlow M (2013a) The regional forcing of northern hemisphere drought during recent warm tropical west Pacific Ocean La Niña events. *Clim Dyn*. <https://doi.org/10.1007/s00382-013-1799-4>
- Hoell A, Barlow M, Saini R (2013b) Intraseasonal and seasonal-to-interannual indian ocean convection and hemispheric teleconnections. *J Clim* 26:8850–8867
- Hoell A, Funk C, Barlow M (2014) La Niña diversity and Northwest Indian Ocean Rim teleconnections. *Clim Dyn* 43:2707–2724
- Hoell A, Shukla S, Barlow M, Cannon F, Kelley C, Funk C (2015a) The forcing of monthly precipitation variability over southwest Asia during the boreal cold season. *J Clim* 28:7038–7056. <https://doi.org/10.1175/JCLI-D-14-00757.1>
- Hoell A, Funk C, Barlow M (2015b) The forcing of southwestern Asia teleconnections by low-frequency sea surface temperature variability during boreal winter. *J Clim* 28:1511–1526
- Hoell A, Barlow M, Cannon F, Xu T (2017a) Oceanic origins of historical southwest Asia precipitation during the boreal cold season. *J Clim* 30:2885–2903
- Hoell A, Funk C, Barlow M, Cannon F (2017b) A physical model for extreme drought over southwest Asia. *Climate Extremes: Patterns and Mechanisms*, *Geophys Monogr Vol 226 American Geophysical Union*, pp 283–298
- Hoell A, Barlow M, Xu T, Zhang T (2018a) Cold season southwest asia precipitation sensitivity to El Niño-southern oscillation events. *J Clim* 31:4463–4482
- Hoell A, Cannon F, Barlow M (2018b) Middle east and southwest Asia daily precipitation characteristics associated with the Madden Julian oscillation during boreal winter. *J Clim*. <https://doi.org/10.1175/JCLI-D-18-0059.1>
- Immerzeel WW, Wanders N, Lutz AF, Shea JM, Bierkens MFP (2015) Reconciling high-altitude precipitation in the upper Indus basin with glacier mass balances and runoff. *Hydrol Earth Syst Sci* 19:4673–4687
- Jiang X, Yang S, Li Y, Kumar A, Liu X, Zuo Z, Jha B (2013) Seasonal-to-interannual prediction of the Asian summer monsoon in the NCEP climate forecast system version 2. *J Clim* 26:3708–3727. <https://doi.org/10.1175/JCLI-D-12-00437.1>
- Kanamitsu M et al (2002) NCEP-DEO AMIP-II reanalysis (R-2). *Bull Am Met Soc* 83:1631–1643
- Kang IS, Shukla J (2006) Dynamic seasonal prediction and predictability of the monsoon. In: Wang B (ed) *The Asian monsoon*. Springer-Paraxis, Chichester
- Kang IS, Rashid IU, Kucharski F, Almouzaoui M, AlKhalaf AA (2015) Multi-decadal changes in the relationship between ENSO and wet-season precipitation in the Arabian Peninsula. *J Clim* 28:4743–4752
- Kirtman BP, Min D (2009) Multimodel ensemble ENSO prediction with CCSM and CFS. *Mon Weather Rev* 137:2908

- Kirtman et al (2014) The North American Multimodel Ensemble: phase-1 seasonal-to-interannual prediction, phase-2 toward developing intraseasonal prediction. *Bull Am Meteorol Soc* 95:585–601
- Lu B, Scaife AA, Dunstone N, Smith D, Ren HL, Liu Y, Eade R (2017) Skillful seasonal predictions of winter precipitation over southern China. *Environ Res Lett* 12:074021. <https://doi.org/10.1088/1748-9326/aa739a>
- Lutz AF, Immerzeel WW, Shrestha AB, Bierkens MFP (2014) Consistent increase in High Asia's runoff due to increasing glacier melt and precipitation. *Nat Clim Chang* 4:587–592
- Madrigal J, Solera A, Almiñana SS, Arquiola JP, Andreu J, Sonia TSQ (2018) Skill assessment of a seasonal forecast model to predict drought events for water resource systems. *J Hydrol* 564:574–587. <https://doi.org/10.1016/j.jhydrol.2018.07.046>
- Ogutu GEO, Franssen WHP, Supit I, Omondi P, Hutjes RWA (2017) Skill of ECMWF system-4 ensemble seasonal climate forecasts for East Africa. *Int J Climatol* 37:2734–2756. <https://doi.org/10.1002/joc.4876>
- Ogutu GEO, Franssen WHP, Supit I, Omondi P, Hutjes RWA (2018) Probabilistic maize yield prediction over East Africa using dynamic ensemble seasonal climate forecasts. *Agric For Meteorol* 250:243–261. <https://doi.org/10.1016/j.agrfor.2017.12.256>
- Palazzi E, Von Hardenberg J, Provenzale A (2013) Precipitation in the Hindu-Kush Karakoram Himalaya: observations and future scenarios. *J Geophys Res Atmos* 118:85–100
- Palmer TN et al (2004) Development of a European multimodel ensemble system for seasonal-to-interannual prediction (DEMETER). *Bull Am Meteorol Soc* 85:853–872
- Rana S, McGregor J, Renwick J (2017) Wintertime precipitation climatology and ENSO sensitivity over central southwest Asia. *Int J Climatol* 37:1494–1509. <https://doi.org/10.1002/joc.4793>
- Rana S, Renwick J, McGregor J, Singh A (2018) Seasonal prediction of winter precipitation anomalies over central Southwest Asia: a canonical correlation analysis approach. *J Clim* 31:727–741. <https://doi.org/10.1175/JCLI-D-17-0131.1>
- Rehman A, Jingdong L, Shahzad B, Chandio A, Hussain I, Nabi G, Iqbal MS (2016) Economic perspectives of major field crops of Pakistan: an empirical study. *Pac Sci Rev B Humanit Soc Sci* 1(3):145–158. <https://doi.org/10.1016/j.psr.2016.09.002>
- Reynolds RW, Rayner NA, Smith TM, Stokes DC, Wang W (2002) An improved in situ and satellite SST analysis for climate. *J Clim* 15:1609–1625
- Rowell DP (1998) Assessing potential seasonal predictability with an ensemble of multi-decadal GCM simulations. *J Clim* 11:109–120
- Rowell DP, Folland CK, Maskell K, Ward MN (1995) Variability of summer rainfall over Tropical North Africa (1906–92) observations and modelling. *Q J R Meteorol Soc* 121:669–704
- Saha SK et al (2014) The NCEP climate forecast system version 2. *J Clim* 27:2185–2208
- Saha SK, Pokhrel S, Salunke K, Dhakate A, Chaudhari HS, Rahman H, Sikka DR (2016) Potential predictability of Indian summer monsoon rainfall in NCEP CFSv2. *J Adv Model Earth Syst* 8:96–120
- Sarfaraz S, Khan TMA (2015) A study of anomalous wet and dry years in the winter precipitation of Pakistan and potential crop yields vulnerability. *J Basic Appl Sci* 11:637–644
- Schepen A, Wang QJ, Everingham Y (2016) Calibration, bridging, and merging to improve GCM seasonal temperature forecasts in Australia. *Mon Weather Rev* 144:2421–2441
- Vecchi GA et al (2014) On the seasonal forecasting of regional tropical cyclone activity. *J Clim* 27:7994–8016
- Vernieres G et al (2012) The GEOS-ODAS, description and evaluation. NASA technical report series on global modeling and data assimilation, NASA/TM–2012–104606, vol 30
- Viel C, Beaulant AL, Soubeyrou JM, Céron JP (2016) How seasonal forecast could help a decision maker: an example of climate service for water resource management. *Adv Sci Res* 13:51–55. <https://doi.org/10.5194/asr-13-51-2016>
- Wang B et al (2009) Advance and prospectus of seasonal prediction: assessment of the APCC/CliPAS 14-model ensemble retrospective seasonal prediction (1980–2004). *Clim Dyn* 33:93–117
- Wilks DS (2006) *Statistical methods in the atmospheric sciences* (Chapter No. 5), 2nd edn. Elsevier, New York
- Xue Y, Huang B, Hu ZZ, Kumar A, Wen C, Behringer D (2011) An assessment of oceanic variability in the NCEP climate forecast system reanalysis. *Clim Dyn* 37:2511–2539

Publisher's Note Springer Nature remains neutral with regard to jurisdictional claims in published maps and institutional affiliations.